Spin-lattice relaxation of individual solid-state spins

A. Norambuena, E. Muñoz, H. T. Dinani, A. Jarmola, P. Maletinsky, D. Budker, and J. R. Maze

Phys. Rev. B **97**, 094304 — Published 20 March 2018

DOI: 10.1103/PhysRevB.97.094304

Spin-lattice relaxation of individual solid-state spins

A. Norambuena[1,2], E. Muñoz[1,2], H. T. Dinani[1], A. Jarmola[3], P. Maletinsky[4], D. Budker[3,5,6], and J. R. Maze[1,2]

[1] *Faculty of Physics, Pontificia Universidad Católica de Chile, Avda. Vicuña Mackenna 4860, Santiago, Chile*
[2] *Center for Nanotecnology and Advanced Materials CIEN-UC, Pontificia Universidad Católica de Chile, Avda. Vicuña Mackenna 4860, Santiago, Chile*
[3] *Department of Physics, University of California, Berkeley 94720-7300, USA*
[4] *Department of Physics, University of Basel, Klingelbergstrasse 82, CH-4056 Basel, Switzerland*
[5] *Helmholtz Institute, Johannes Gutenberg University, 55128 Mainz*
[6] *Nuclear Science Division, Lawrence Berkeley National Laboratory*

(Dated: March 5, 2018)

Understanding the effect of vibrations on the relaxation process of individual spins is crucial for implementing nano systems for quantum information and quantum metrology applications. In this work, we present a theoretical microscopic model to describe the spin-lattice relaxation of individual electronic spins associated to negatively charged nitrogen-vacancy centers in diamond, although our results can be extended to other spin-boson systems. Starting from a general spin-lattice interaction Hamiltonian, we provide a detailed description and solution of the quantum master equation of an electronic spin-one system coupled to a phononic bath in thermal equilibrium. Special attention is given to the dynamics of one-phonon processes below 1 K where our results agree with recent experimental findings and analytically describe the temperature and magnetic-field scaling. At higher temperatures, linear and second-order terms in the interaction Hamiltonian are considered and the temperature scaling is discussed for acoustic and quasi-localized phonons when appropriate. Our results, in addition to confirming a T^5 temperature dependence of the longitudinal relaxation rate at higher temperatures, in agreement with experimental observations, provide a theoretical background for modeling the spin-lattice relaxation at a wide range of temperatures where different temperature scalings might be expected.

PACS numbers:

I. INTRODUCTION

The negatively charged nitrogen-vacancy (NV^-) center in diamond is a promising solid-state system with remarkable applications in quantum sensing with atomic-scale spatial resolution[1,2], fluorescent marking of biological structures[3–5], single photon sources[6], and quantum communications[7]. However, most of these quantum-based applications crucially depend on the longitudinal ($1/T_1$) and transverse ($1/T_2$) spin relaxation rates associated with the ground state spin degree of freedom[8].

From experiments and theory, we know that lattice phonons in diamond are important for the spin-lattice relaxation dynamics of the spin degree of freedom of the NV^- center, and that the temperature plays a fundamental role in this relaxation process[8–12]. Phonons can be understood as collective quantum vibrational excitations that propagate through the lattice and directly interact with the orbital states of the point defect. The intensity of this interaction depends on the electron-phonon coupling between the defect and all possible phonon modes in the lattice (acoustic, optical and quasi-localized phonon modes)[13–15]. Theoretical and numerical studies show that the strain field of the diamond lattice and perturbative corrections given by the spin-orbit and spin-spin interactions introduce interesting spin-phonon dynamics between the ground state spin degree of freedom of the NV^- center and lattice phonons[16,17].

Several theoretical works have addressed the problem of finding the relaxation rate by considering the interaction between the spin degree of freedom with two-phonon Raman[18,19] and Orbach-type[20] processes. In general, the problem of estimating the thermal dependence of each relaxation process is translated into the problem of calculating the transition rates predicted by the Fermi golden rule for different phonon processes[12,18–21]. Using this reasoning, it is reported that the second-order Raman process induced by a linear spin-phonon interaction leads to $1/T_1 \propto T^5$[19], while the first-order Raman process induced by a quadratic spin-phonon interaction leads to $1/T_1 \propto T^7$[18], where T is the environment temperature.

The ground triplet state of the NV^- center in diamond has a natural zero-field splitting $D/2\pi = 2.87$ GHz originated from the dipole-dipole interaction between electronic spins[22,23]. This energy gap is low compared to typical optical phonon energies $\omega_{\rm ph}/2\pi \sim$ 15-40 THz and sets a characteristic thermal gap associated with the spin system $T_{\rm gap} = \hbar D/k_B \approx 0.14$ K. Experimental observations at high temperatures, from 300 K to 475 K, have shown that different samples with different NV^- center concentrations present a dominant two-phonon Raman process that leads to $(1/T_1)_{\rm Raman} \propto T^5$[8,11]. At low temperatures, between 4 K and 100 K, the relaxation rate is dominated by Orbach and spin-bath interactions. The former is associated with a quasi-localized phonon mode with energy $\omega_{\rm loc} \approx 73$ meV[8,24] and contributes with a temperature dependence relaxation rate $(1/T_1)_{\rm Orbach} \propto (\exp(\hbar\omega_{\rm loc}/k_BT) - 1)^{-1}$. This, closely matches the numerical vibrational resonance predicted by *ab initio* studies[13]. Meanwhile, it is observed that dipole-

dipole interactions between neighboring spins lead to a constant sample-dependent relaxation rate which dominates at this temperature range[8]. In contrast, at lower temperatures (below 1 K) recent experimental observations and *ab initio* calculations concluded that the longitudinal relaxation rate is dominated by single-phonon processes, and is given by $(1/T_1) \propto \Gamma_0 \left(1 + 3\bar{n}(T)\right)$, where $\Gamma_0 = 3.14 \times 10^{-5}$ s^{-1}, and $\bar{n}(T) = (\exp(\hbar D/k_B T) - 1)^{-1}$ is the mean number of phonons at the zero-field splitting frequency[12]. However, a microscopic model that predicts the temperature dependence of the longitudinal relaxation rate for a wide range of temperatures, to the best of our knowledge, is still missing.

Here, we present a microscopic model for the spin-lattice relaxation dynamics associated with the ground state of the NV$^-$ center in diamond. In our model, we introduce a general spin-phonon Hamiltonian to describe the spin relaxation dynamics using the quantum master equation associated with the electronic spin degree of freedom under the effect of a phononic bath. We focus on the estimation of the longitudinal relaxation rate by evaluating the rate of the Fermi golden rule transitions to first and second-order considering the effect of acoustic and quasi-localized phonons. In Sec. II, we give the Hamiltonian of the whole system and introduce the spin-phonon interaction between the triplet state of the spin degree of freedom and lattice vibrations, by considering one-phonon and two-phonon interactions. Section III introduces the phonon relaxation rates for one-phonon and two-phonon processes, by using the Fermi golden rule, the Debye approximation, and a model for strong interactions with quasi-localized phonon modes. In Sec. IV we introduce the quantum master equation associated with the spin-lattice relaxation dynamics of the ground state and include the role of a stochastic magnetic noise. Finally, in Section V we discuss the longitudinal relaxation rate at low and high-temperature regimes and the role of a static magnetic field on the relaxation rate for low temperatures.

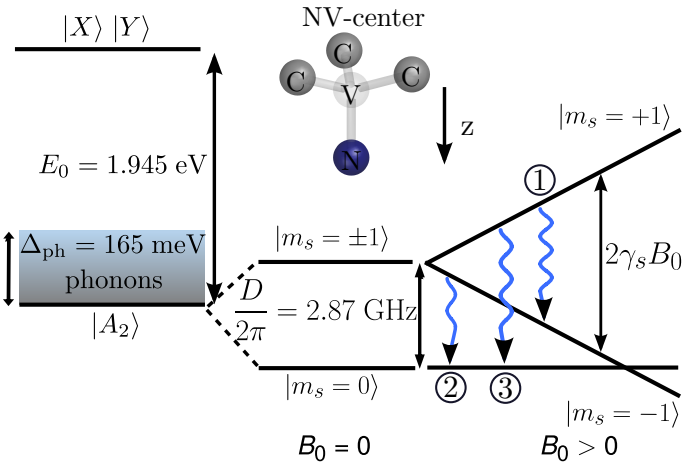

FIG. 1. The energy levels and the atomic structure of the NV$^-$ center are shown. Here, $|X\rangle$ and $|Y\rangle$ are the orbital degenerate excited states, and $|A_2\rangle$ is the orbital ground state. The zero-phonon line energy is given by $E_0 = 1.945$ eV. The spin triplet states are represented by $|m_s = 0\rangle$ and $|m_s = \pm 1\rangle$. Such spin states are separated by the zero-field splitting constant $D/2\pi = 2.87$ GHz and the static magnetic field which we have assumed is aligned along the symmetry axis of the center. Phonons are represented by a continuous band that interacts with the ground state and its transitions are represented by the labels (1), (2), and (3).

II. SPIN DEGREE OF FREEDOM AND PHONONS

We consider a system composed of a single NV$^-$ center in diamond interacting with lattice phonons. In this scenario, local vibrations induce a mixing between orbital states of the defect by means of the electron-phonon interaction. This phonon-induced mixing effect generates an effective interaction between the spin degree of freedom and lattice phonons. In order to model the spin-phonon relaxation dynamics, we use the following Hamiltonian

$$\hat{H} = \hat{H}_{\rm NV} + \hat{H}_{\text{s-ph}} + \hat{H}_{\rm ph}, \tag{1}$$

where the first, second and third terms represent the ground state spin Hamiltonian of the NV$^-$ center, the interaction Hamiltonian between the spin state and lattice phonons, and the phonon bath, respectively.

The NV$^-$ center is composed of a substitutional nitrogen atom next to a vacancy in a diamond lattice. The symmetry of the center is captured by including the three carbon atoms adjacent to the vacancy[25]. The atomic configuration of this point defect is associated with the C_{3v} symmetry group. The electronic structure of this point defect is modeled as a two electron-hole system with electronic spin $S = 1$. In this representation, the electronic wavefunctions of the excited and ground state are linear combinations of two-electron wave functions[26], where the single-electron orbitals of the NV$^-$ center can be written in terms of the carbon and nitrogen dangling bonds[27,29]. In the absence of external perturbations, such as lattice distortions or electromagnetic fields, the orbital excited states $|X\rangle$ and $|Y\rangle$ are degenerate due to the C_{3v} symmetry and belong to the irreducible representation E. Meanwhile, the orbital ground state $|A_2\rangle$ belongs to the irreducible representation A_2.

In the presence of a static magnetic field B_0 along the z axis, the spin Hamiltonian of the NV$^-$ center is given by ($\hbar = 1$)

$$\hat{H}_{\rm NV} = D S_z^2 + \gamma_s B_0 S_z, \tag{2}$$

where $\mathbf{S} = (S_x, S_y, S_z)$ are the Pauli matrices for $S = 1$ (dimensionless), $D/2\pi = 2.87$ GHz is the zero-field splitting constant, and $\gamma_s/2\pi \approx 2.8$ MHz/G is the gyromagnetic ratio. Figure. 1 shows the energy diagram of the system, including the orbital states, spin degrees of freedom and the atomic configuration of the NV$^-$ center.

Quantum systems with spin $S = 1$ are traditionally called non-Kramers systems[30,31]. Interestingly, there is a non-trivial connection between the spin number and

the temperature dependence of the relaxation rate[19,20,27]. Therefore, in order to obtain the correct temperature dependence of the spin relaxation rate of the ground triplet state of the NV^- center we consider the most general spin-phonon interaction Hamiltonian for spin $S = 1$ systems given by[30]

$$\hat{H}_{\text{s-ph}} = E_z S_z^2 + E_x \left(S_x^2 - S_y^2\right) + E_y \left(S_x S_y + S_y S_x\right) + E_{x'} \left(S_x S_z + S_z S_x\right) + E_{y'} \left(S_y S_z + S_z S_y\right), \quad (3)$$

where the operators $E_z, E_x, E_y, E_{x'}$ and $E_{y'}$ have units of energy. In addition, the operators E_x, $E_{x'}$, E_y, and $E_{y'}$ belong to the irreducible representation E, while the operator E_z is characterized by the irreducible representation A_1[30]. Physically, the E_i operators can be derived from perturbative corrections of the spin-spin and spin-orbit interactions due to the effect of the strain field[17]. These operators are proportional to the nuclear displacements, and therefore, can be quantized using phonon modes[17]. In order to introduce these quantized vibrations, we expand the E_i operators in terms of lattice phonon-mode operators classified by each symmetry, including the linear and the quadratic terms, as the following

$$E_i = \sum_{k \in E} \lambda_{k,i} \hat{x}_k + \sum_{k \otimes k' \in E} \lambda_{kk',i} \hat{x}_k \hat{x}_{k'}, \quad i \neq z \quad (4)$$

$$E_z = \sum_{k \in A_1} \lambda_{k,z} \hat{x}_k + \sum_{k \otimes k' \in A_1} \lambda_{kk',z} \hat{x}_k \hat{x}_{k'}. \quad (5)$$

Here, $\lambda_{k,i}$ and $\lambda_{kk',i}$ are the linear and quadratic spin-phonon coupling constants, respectively. The operator $\hat{x}_k$ is given by $\hat{x}_k = \hat{b}_k + \hat{b}_k^\dagger$ where $\hat{b}_k$ and $\hat{b}_k^\dagger$ are the boson annihilation and creation operators, respectively satisfying $[\hat{b}_k, \hat{b}_{k'}^\dagger] = \delta_{k,k'}$. The linear term given in Eqs. (4) and (5) has the same symmetry as the corresponding E_i operators, and phonons with these symmetry are considered in the summation. In the quadratic term we are considering combinations of phonons such that the product belongs to the irreducible representation E or A_1. As a consequence of the multiplication rules $A_2 \otimes A_2 = A_1$ and $A_2 \otimes E = E$, phonon modes with A_2 symmetry only contribute to the quadratic term. Therefore, the most general spin-phonon Hamiltonian for a system with spin $S = 1$, is given by

$$\hat{H}_{\text{s-ph}} = \sum_i \left[\sum_{k \in \Gamma_i} \lambda_{k,i} \hat{x}_k + \sum_{k \otimes k' \in \Gamma_i} \lambda_{kk',i} \hat{x}_k \hat{x}_{k'} \right] \hat{F}_i(\mathbf{S}), \quad (6)$$

where $i = x, y, x', y', z$ is the spin label, $\Gamma_{x,y,x',y'} = E$ and $\Gamma_z = A_1$ are the irreducible representations of the C_{3v} point group. The spin functions are given by $\hat{F}_x(\mathbf{S}) = S_x^2 - S_y^2, \hat{F}_y(\mathbf{S}) = S_x S_y + S_y S_x, \hat{F}_{x'}(\mathbf{S}) = S_x S_z + S_z S_x, \hat{F}_{y'}(\mathbf{S}) = S_y S_z + S_z S_y$, and $\hat{F}_z(\mathbf{S}) = S_z^2$.

Using the spin basis that diagonalizes the spin Hamiltonian given in Eq. (2), i.e., $|m_s = 1\rangle = (1,0,0), |m_s = 0\rangle = (0,1,0)$, and $|m_s = -1\rangle = (0,0,1)$ we explicitly obtain

$$\hat{F}_x(\mathbf{S}) = \begin{pmatrix} 0 & 0 & 1 \\ 0 & 0 & 0 \\ 1 & 0 & 0 \end{pmatrix}, \; \hat{F}_{x'}(\mathbf{S}) = \frac{1}{\sqrt{2}} \begin{pmatrix} 0 & 1 & 0 \\ 1 & 0 & -1 \\ 0 & -1 & 0 \end{pmatrix}, \quad (7)$$

$$\hat{F}_y(\mathbf{S}) = \begin{pmatrix} 0 & 0 & -i \\ 0 & 0 & 0 \\ i & 0 & 0 \end{pmatrix}, \; \hat{F}_{y'}(\mathbf{S}) = \frac{1}{\sqrt{2}} \begin{pmatrix} 0 & -i & 0 \\ i & 0 & i \\ 0 & -i & 0 \end{pmatrix}, \quad (8)$$

$$\hat{F}_z(\mathbf{S}) = \begin{pmatrix} 1 & 0 & 0 \\ 0 & 0 & 0 \\ 0 & 0 & 1 \end{pmatrix}. \quad (9)$$

We observe that only the terms $\hat{F}_x(\mathbf{S})$ and $\hat{F}_y(\mathbf{S})$ induce spin transitions between the states $m_s = +1$ and $m_s = -1$, where the selection rule is $\Delta m_s = \pm 2$. On the other hand, the terms $\hat{F}_{x'}(\mathbf{S})$ and $\hat{F}_{y'}(\mathbf{S})$ induce spin transitions between $m_s = \pm 1$ and $m_s = 0$, in this case the selection rule is $\Delta m_s = \pm 1$.

Finally, the phonon Hamiltonian can be written as

$$\hat{H}_{\text{ph}} = \sum_k \hbar \omega_k \hat{b}_k^\dagger \hat{b}_k, \quad (10)$$

where ω_k is the frequency of each vibrational mode of the lattice (including the color center), and the summation takes into account the contribution of all phonon modes of the diamond lattice. In the next section, we will introduce the phonon-induced spin relaxation rates and the temperature dependence associated to the spin-phonon Hamiltonian given in Eq. (6) by considering the effect of acoustic and quasi-localized phonons in thermal equilibrium. We will show that the dimension and the symmetry of the lattice play a fundamental role in the temperature dependence of the longitudinal relaxation rate for two-phonon processes.

III. FERMI GOLDEN RULE AND PHONON-INDUCED SPIN RELAXATION RATES

In order to formally introduce the phonon-induced relaxation rates, we use the Fermi golden rule to first and second order by using the spin-phonon Hamiltonian given in Eq. (6). Using this procedure, it is possible to model first and second-order Raman-like processes, as well as direct absorption and emission associated with one-phonon processes. In particular, the energies associated with the spin transitions in the ground state of the NV^- center are given by $\omega_1 = 2\gamma_s B_0$, $\omega_2 = D + \gamma_s B_0$, and $\omega_3 = D - \gamma_s B_0$. For typical magnitudes of the static magnetic field $B_0 \sim 0 - 2000$ G and taking into account the zero field splitting constant $D/2\pi = 2.87$ GHz, we obtain that $\omega_1 \sim 0 - 11.2$ GHz, $\omega_{2,3} \sim 2.87 - 8.47$ GHz. These are the typical energies of acoustic phonons which belong to the linear branch of the phonon dispersion relation for diamond[28]. Acoustic phonons in diamond have energies of the order of $\omega_{\text{acous}} \sim 0 - 10$ THz. Therefore, the main fraction of acoustic phonons satisfy the frequency condition $\omega_{\text{acous}} \gg \omega_i$.

For the case of Raman-like processes the frequency condition is $\omega_{\text{ph},1}-\omega_{\text{ph},2}=\omega_i$ $(i=1,2,3)$. Due to the condition $\omega_{\text{acous}}\gg\omega_i$ we assume in our model that the most significant contribution to two-phonon processes comes from acoustic phonons that satisfy $\omega_{\text{ph},1}\gg\omega_i$ and $\omega_{\text{ph},2}\gg\omega_i$. On the other hand, high energy phonons in diamond, with frequencies of the order of $\omega_{\text{ph}}\sim 15-40$ THz, can be included by considering the strong interaction with quasi-localized phonons. Therefore, in what follows we will consider the contribution of acoustic and quasi-localized phonons.

A. One-phonon processes: acoustic phonons

In the case of one-phonon processes, we need to distinguish between the absorption and the emission of a particular phonon mode with frequency ω_k, which must be resonant with a transition between the spin energy levels of the NV^- center in diamond. In order to introduce the temperature, we assume a phonon environment in thermal equilibrium, i.e., phonons that satisfy the Bose-Einstein distribution. Thus, we have $\langle\hat{b}_k^\dagger\hat{b}_k\rangle=n(\omega_k)$ and $\langle\hat{b}_k\hat{b}_k^\dagger\rangle=1+n(\omega_k)$, where $n(\omega_k)=\left[\exp\left(\hbar\omega_k/k_BT\right)-1\right]^{-1}$ is the mean number of phonons at thermal equilibrium with k_B and $\hbar$ being the Boltzmann and Planck constant, respectively.

For one-phonon processes the absorption and emission transition rates associated with the spin transition $|m_s\rangle\to|m_s'\rangle$ are given by the first order Fermi golden rule as

$$\Gamma_{\text{abs}}^{m_s\to m_s'}=\frac{2\pi}{\hbar^2}\sum_k\left|\langle m_s',n_k-1\left|\hat{H}_{\text{s-ph}},\right|m_s,n_k\rangle\right|^2\times\delta(\omega_{m_s',m_s}-\omega_k),\tag{11}$$

$$\Gamma_{\text{em}}^{m_s\to m_s'}=\frac{2\pi}{\hbar^2}\sum_k\left|\langle m_s',n_k+1\left|\hat{H}_{\text{s-ph}}\right|m_s,n_k\rangle\right|^2\times\delta(\omega_{m_s',m_s}-\omega_k),\tag{12}$$

where $\omega_{m_s',m_s}=\omega_{m_s'}-\omega_{m_s}$ is the frequency difference between the spin sub-levels, and $|n_k\rangle$ is the number of phonons in the mode k (Fock state). Using the spin-phonon Hamiltonian given in Eq. (6), the spin relaxation rates associated with one-phonon processes are given by

$$\Gamma_{\text{abs}}^{1,\text{1-ph}}=\frac{2\pi}{\hbar^2}n(\omega_1)J_1(\omega_1),\quad\Gamma_{\text{em}}^{1,\text{1-ph}}=\frac{2\pi}{\hbar^2}\left(n(\omega_1)+1\right)J_1(\omega_1),\tag{13}$$

$$\Gamma_{\text{abs}}^{2,\text{1-ph}}=\frac{\pi}{\hbar^2}n(\omega_2)J_2(\omega_2),\quad\Gamma_{\text{em}}^{2,\text{1-ph}}=\frac{\pi}{\hbar^2}\left(n(\omega_2)+1\right)J_2(\omega_2),\tag{14}$$

where the superscript "1" and "2" represent the spin transitions $|m_s=-1\rangle\leftrightarrow|m_s=1\rangle$ and $|m_s=0\rangle\leftrightarrow|m_s=+1\rangle$, respectively. Here, $J_1(\omega)$ and $J_2(\omega)$ are the spectral density functions

$$J_1(\omega)=\sum_{k\in E}\left(\lambda_{k,x}^2+\lambda_{k,y}^2\right)\delta(\omega-\omega_k),\tag{15}$$

$$J_2(\omega)=\sum_{k\in E}\left(\lambda_{k,x'}^2+\lambda_{k,y'}^2\right)\delta(\omega-\omega_k),\tag{16}$$

where $\lambda_{k,i}$ are the linear spin-phonon coupling constants, ω_k are the phonon frequencies, and both summations consider the contribution of E phonons. For the transition $|m_s=0\rangle\leftrightarrow|m_s=-1\rangle$ the gap frequency $\omega_3=D-\gamma_sB_0$ can be positive or negative depending on the strength of the external magnetic field B_0. For $\omega_3>0$ the absorption and emission relaxation rates are given by

$$\Gamma_{\text{abs}}^{3,\text{1-ph}}=\frac{\pi}{\hbar^2}n(\omega_3)J_2(\omega_3),\tag{17}$$

$$\Gamma_{\text{em}}^{3,\text{1-ph}}=\frac{\pi}{\hbar^2}(n(\omega_3)+1)J_2(\omega_3),\tag{18}$$

where the superscript "3" represents the spin transition $|m_s=0\rangle\leftrightarrow|m_s=-1\rangle$. In this case, the spin state $|m_s=0\rangle$ is the lowest spin energy level and the absorption is defined by the transition $|m_s=0\rangle\to|m_s=-1\rangle$. In the opposite case, i.e., when $\omega_3<0$, the relaxation rates can be written as the following

$$\Gamma_{\text{abs}}^{3,\text{1-ph}}=\frac{\pi}{\hbar^2}n(|\omega_3|)J_2(|\omega_3|),\tag{19}$$

$$\Gamma_{\text{em}}^{3,\text{1-ph}}=\frac{\pi}{\hbar^2}(n(|\omega_3|)+1)J_2(|\omega_3|).\tag{20}$$

In this case the spin state $|m_s=-1\rangle$ is the lowest spin energy level, and the absorption is defined by the transition $|m_s=-1\rangle\to|m_s=0\rangle$. Figure 2 shows the phonon-induced spin relaxation rates associated with the ground triplet state of the NV^- center as a function of the external magnetic field B_0. The absorption and emission relaxation rates associated with the transitions $|m_s=0\rangle\leftrightarrow|m_s=-1\rangle$ are shown only for the case $\omega_3<0$. The total phonon-induced spin relaxation rate associated with one-phonon processes is defined as the sum of the absorption and emission transition rates of each process, and is given by

$$\Gamma_{\text{1-ph}}=\sum_{i=1}^{3}\left(\Gamma_{\text{abs}}^{i,\text{1-ph}}+\Gamma_{\text{em}}^{i,\text{1-ph}}\right)=\sum_{i=1}^{3}A_i\coth\left(\frac{\hbar\omega_i}{2k_BT}\right).\tag{21}$$

This total phonon-induced spin relaxation rate will be relevant for the general solution associated with the populations of the spin states and the observable $\langle S_z(t)\rangle$ (see Section V B and Eqs. (71) and (74)). In addition, this transition rate, i.e., the sum of absorption and emission of all the transitions, is the rate that limits the coherence time T_2[32]. The parameters A_i depend on the value of the spectral density function at the resonant frequencies, i.e., $A_1=2\pi J_1(\omega_1)$, $A_2=\pi J_2(\omega_2)$, and $A_3=\pi J_2(|\omega_3|)$.

In the limit of continuous frequency, i.e., $\omega_k\to\omega$, we can introduce the following scaling for the linear spin-phonon coupling constants[34]:

$$\lambda_{k,i}\to\lambda_i(\omega)=\lambda_{0i}\left(\frac{\omega}{\omega_D}\right)^\nu,\qquad 0\le\omega\le\omega_D,\tag{22}$$

where $\lambda_i(\omega)$ is the one-phonon coupling constant for acoustic phonons, $\lambda_{0i}=\lambda_i(\omega_D)$ is the strength of the one-phonon coupling constant at the Debye frequency $\omega_D=\left(3/(4\pi n)\right)^{1/3}v_s$, where n is the atom density, and v_s is the

speed of sound. For the diamond lattice the Debye frequency is given by $\omega_D/2\pi = 38.76$ THz[35]. The parameter ν is a phenomenological parameter that models the strength of the coupling for acoustic phonons and depends on the symmetry of the lattice. In the absence or presence of cubic symmetry we have $\nu = 1/2$ or $\nu = 3/2$, respectively[34]. For the NV$^-$ center in diamond we use the value $\nu = 1/2$, because of the presence of the color center with C_{3v} symmetry that breaks the symmetry of the whole system (lattice and point defect).

We introduce the density of states for acoustic phonons with E symmetry for a d-dimensional lattice, with a dispersion relation $\omega_k = v_s|\mathbf{k}|$ in the Debye approximation ($\omega \leq \omega_D = v_s k_D$):

$$\begin{aligned}\mathcal{D}^{(d)}(\omega) &= \Omega \int \frac{d^d k}{(2\pi)^d}\delta(\omega - v_s|\mathbf{k}|) \\ &= \frac{\Omega}{(2\pi)^d}\int d\hat{\Omega}_d \int_0^{k_D} dk\, k^{d-1}\delta(\omega - v_s k) \\ &= D_0 \left(\frac{\omega}{\omega_D}\right)^{d-1} \Theta(\omega_D - \omega). \end{aligned} \tag{23}$$

Here, we have used d-dimensional spherical coordinates with measure $d^d k = d\hat{\Omega}_d dk k^{d-1}$, with $\hat{\Omega}_d$ the solid angle in d-dimensions and $\omega_D = v_s k_D$ the Debye frequency for the diamond lattice. In the last line, we have defined the positive normalization constant $D_0 = \Omega\hat{\Omega}_d\omega_D^{d-1}/((2\pi)^d v_s^d) > 0$, for $d = 1, 2, 3$ the dimension of the lattice. In Eq. (23) we have taken the continuum limit of the sum, Ω is the volume of a unit cell, $v_s = 1.2 \times 10^4$ m/s is the speed of sound in a diamond lattice, and $\omega_D = v_s k_D$ is the Debye frequency for the diamond lattice. The frequency domain is truncated in the upper limit to the Debye frequency by the Heaviside function $\Theta(\omega_D - \omega)$. For a three-dimensional lattice we obtain $D_0 = \Omega\omega^2/(2\pi^2 v_s^3)$. In the limit of continuous frequency and considering a three dimensional lattice, the spectral density functions can be written as

$$\begin{aligned} J_1(\omega) &= \sum_{k\in E}\left[\lambda_x^2(\omega_k) + \lambda_y^2(\omega_k)\right]\delta(\omega - \omega_k) \\ &\to \Omega\int \frac{d^3k}{(2\pi)^3}\left[\lambda_x^2(\omega_k) + \lambda_y^2(\omega_k)\right]\delta(\omega - \omega_k) \\ &= \left[\lambda_x^2(\omega) + \lambda_y^2(\omega)\right]\Omega\int\frac{d^3k}{(2\pi)^3}\delta(\omega - \omega_k) \\ &= [\lambda_x^2(\omega) + \lambda_y^2(\omega)]\mathcal{D}^{(3)}(\omega). \end{aligned} \tag{24}$$

Similar manipulations lead to $J_2(\omega) = [\lambda_{x'}^2(\omega) + \lambda_{y'}^2(\omega)]\mathcal{D}^{(3)}(\omega)$. As a result, the parameters A_i are given by

$$A_1 = \frac{\Omega\left(\lambda_{0x}^2 + \lambda_{0y}^2\right)}{\pi v_s^3\omega_D}\left(2\gamma_s B_0\right)^3, \tag{25}$$

$$A_2 = \frac{\Omega\left(\lambda_{0x'}^2 + \lambda_{0y'}^2\right)}{2\pi v_s^3\omega_D}\left(D + \gamma_s B_0\right)^3, \tag{26}$$

$$A_3 = \frac{\Omega\left(\lambda_{0x'}^2 + \lambda_{0y'}^2\right)}{2\pi v_s^3\omega_D}\left(D - \gamma_s B_0\right)^3. \tag{27}$$

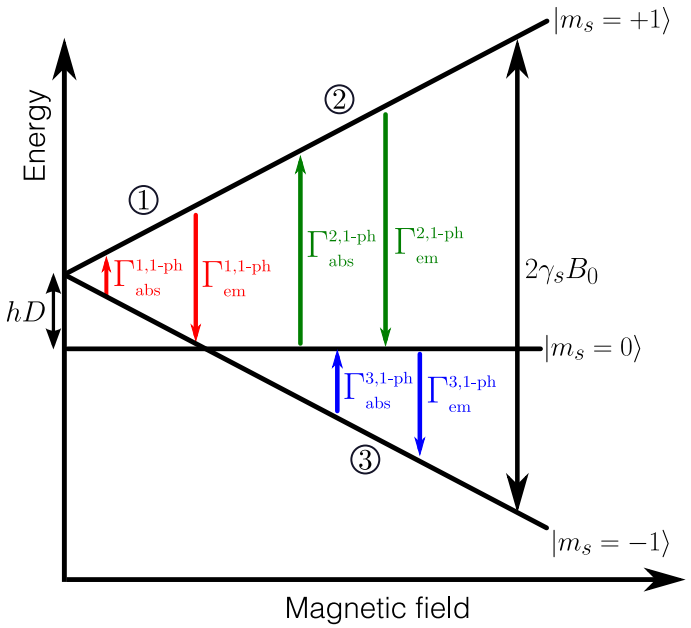

FIG. 2. The solid black lines are the energy levels of the ground triplet state of the NV$^-$ center in diamond as a function of the external magnetic field along the z axis. For a given absorption and emission transition between two spin states $|m_s\rangle$, we observe three different spin relaxation processes represented by colored arrows (1=red, 2=green and 3=blue). The relaxation rates $\Gamma^{i,1\text{-ph}}_{\text{abs}}$ and $\Gamma^{i,1\text{-ph}}_{\text{em}}$ are the absorption and emission spin relaxation rates for one-phonon processes.

Therefore, the available number of phonons in the lattice, the density of phonon states, and the spin-phonon coupling constants will determine the intensity of each transition rate. In this context, the temperature is the control parameter in the laboratory that, at a quantum level, introduces available phonons that collectively act as a source of relaxation. At zero magnetic field, we have $A_1 = 0$ and $A_2 = A_3$. In the high-temperature regime, $k_B T \gg \hbar\omega_i$, the one-phonon spin relaxation rates scales linearly with the temperature, i.e., $\Gamma^{i,1\text{-ph}} \propto T$. In the opposite case, when $k_B T \ll \hbar\omega_i$, the one-phonon spin relaxation rates scales as a constant.

In the next section we introduce the second-order corrections to the Fermi golden rule using both linear and bilinear terms in the spin-phonon interaction Hamiltonian.

B. Two-phonon processes: acoustic phonons

The second-order transition rate associated with the spin transition $|m_s\rangle \to |m_s'\rangle$ is defined as

$$\Gamma_{m_s\to m_s'} = \sum_{k,k'}\sum_{l,l'}\Gamma^{m_s',n_l,n_{l'}}_{m_s,n_k,n_{k'}}, \quad m_s, m_s' = 0, \pm 1, \tag{28}$$

where the sum is over all possible initial and final two-phonon modes, with $|i\rangle = |m_s, n_k, n_{k'}\rangle$ and $|f\rangle = |m_s', n_l, n_{l'}\rangle$ being the initial and final states, respectively. The transition rate inside the sum in Eq. (28) is given by

the Fermi golden rule formula to second-order

$$\Gamma^{m_s',n_l,n_{l'}}_{m_s,n_k,n_{k'}} = \frac{2\pi}{\hbar^2}\Big|V^{m_s',n_l,n_{l'}}_{m_s,n_k,n_{k'}} + \sum_{m_s''=0,\pm1}\sum_{p,p'}\frac{V^{m_s'',n_p,n_{p'}}_{m_s',n_l,n_{l'}}V^{m_s,n_k,n_{k'}}_{m_s'',n_p,n_{p'}}}{E_{m_s,n_k,n_{k'}}-E_{m_s'',n_p,n_{p'}}}\Big|^2 \times\delta(\omega_{m_s',m_s}+n_l\omega_l+n_{l'}\omega_{l'}-n_k\omega_k-n_{k'}\omega_{k'}), \tag{29}$$

where $V_i^j=\langle i|\hat{H}_{\text{s-ph}}|j\rangle$, $|m_s''\rangle$ is the spin state of the intermediate state, and $|n_p\rangle$,$|n_p'\rangle$ are the intermediate phonon states. The resonant frequencies of the system, i.e., $\omega_1\sim 0-11.2$ GHz and $\omega_{2,3}\sim 2.87-8.47$ GHz are very low compared to the frequency of the acoustic phonons in diamond $\omega_{\text{acous}}\sim 0-10$ THz. Therefore, to second-order we assume that the most significant contribution comes from phonons that satisfy the frequency condition $\omega_{k,k'}\gg\omega_{m_s,m_s''}$.

We introduce four different types of two-phonon processes: two-phonon direct transition (Direct), Stokes transition (Stokes), anti-Stokes transition (anti-Stokes), and spontaneous emission followed by absorption (Spont), see Fig. 3. The direct two-phonon transition is characterized by the frequency condition $\omega_k+\omega_{k'}=\omega_{m_s',m_s}$ and its absorption and emission relaxation rates are given by

$$\Gamma^{\text{abs, Direct}}_{m_s\to m_s'}=\sum_{k,k'}\Gamma^{m_s',n_k-1,n_{k'}-1}_{m_s,n_k,n_{k'}}, \tag{30}$$

$$\Gamma^{\text{em, Direct}}_{m_s'\to m_s}=\sum_{k,k'}\Gamma^{m_s,n_k+1,n_{k'}+1}_{m_s',n_k,n_{k'}}. \tag{31}$$

On the other hand, we have the Stokes and Anti-Stokes transitions which are characterized by the frequency condition $\omega_k-\omega_{k'}=\omega_{m_s',m_s}$ and are given by

$$\Gamma^{\text{Stokes}}_{m_s\to m_s'}=\sum_{k,k'}\Gamma^{m_s',n_k-1,n_{k'}+1}_{m_s,n_k,n_{k'}}, \tag{32}$$

$$\Gamma^{\text{Anti-Stokes}}_{m_s'\to m_s}=\sum_{k,k'}\Gamma^{m_s,n_k-1,n_{k'}+1}_{m_s',n_k,n_{k'}}. \tag{33}$$

For the spontaneous emission followed by absorption process we define

$$\Gamma^{\text{abs, Spont}}_{m_s\to m_s'}=\sum_{k,k'}\Gamma^{m_s',n_k+1,n_{k'}-1}_{m_s,n_k,n_{k'}}, \tag{34}$$

$$\Gamma^{\text{em, Spont}}_{m_s'\to m_s}=\sum_{k,k'}\Gamma^{m_s,n_k+1,n_{k'}-1}_{m_s',n_k,n_{k'}}. \tag{35}$$

For acoustic phonon modes, i.e., phonons with a linear dispersion relation $\omega_k=v|\mathbf{k}|$, we can use the Debye model in order to represent two-phonon processes. In order to study the spin-relaxation rate as a function of the dimension of the system, we used the density of phonon states for a d-dimensional lattice given in Eq. (23). We can introduce the following scaling for the quadratic spin-phonon coupling constant for the acoustic phonon modes in the limit of continuous frequency[34]

$$\lambda_{kk',i}\to\lambda_i(\omega,\omega')=\lambda_{00i}\left(\frac{\omega}{\omega_D}\right)^{\nu}\left(\frac{\omega'}{\omega_D}\right)^{\nu}, \tag{36}$$

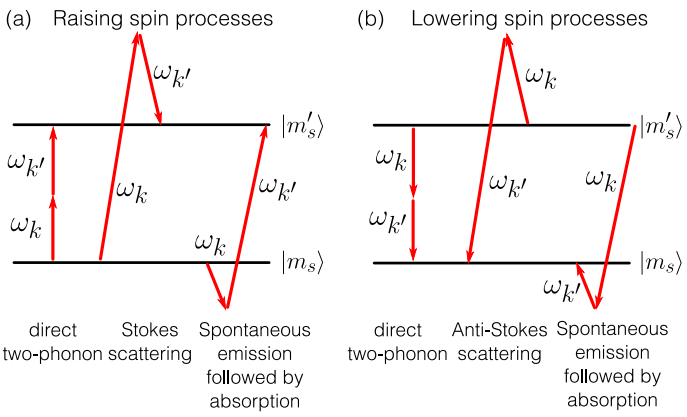

FIG. 3. The red arrows represent the absorption and emission of two phonons between two different spin states $|m_s\rangle$ and $|m_s'\rangle$. The direct two-phonon process is associated to the energy condition $\omega_k+\omega_{k'}=\omega_{m_s',m_s}$, where $\omega_{m_s',m_s}=\omega_{m_s'}-\omega_{m_s}$ is the frequency gap. The Stokes scattering is associated to the energy condition $\omega_k-\omega_{k'}=\omega_{m_s',m_s}$.

where $\lambda_i(\omega,\omega')$ is the two-phonon coupling constant for acoustic phonons, $\lambda_{00i}=\lambda_i(\omega_D,\omega_D)$ is the strength of the two-phonon coupling constant at the Debye frequency ω_D, and $\nu>0$ is a phenomenological factor that models the spin-phonon coupling in the acoustic regime.

Using the second-order Fermi golden rule given in Eq. (A1) and only considering acoustic phonons, we obtain the following absorption and emission transition rates

$$\Gamma^{\text{abs}}_{m_s\to m_s'}=\Gamma^{\text{abs, Direct}}_{m_s\to m_s'}+\Gamma^{\text{Stokes}}_{m_s\to m_s'}+\Gamma^{\text{abs,Spont}}_{m_s\to m_s'}, \tag{37}$$

$$\Gamma^{\text{em}}_{m_s\to m_s'}=\Gamma^{\text{em, Direct}}_{m_s\to m_s'}+\Gamma^{\text{Anti-Stokes}}_{m_s\to m_s'}+\Gamma^{\text{em,Spont}}_{m_s\to m_s'}, \tag{38}$$

where each transition rate is defined as

$$\Gamma^{\text{process}}_{m_s\to m_s'}=a^{\text{process}}_{m_s,m_s'}(x_D)T^{4\nu+2d-3}+b^{\text{process}}_{m_s,m_s'}(x_D)T^{4\nu+2d-2}+c^{\text{process}}_{m_s,m_s'}(x_D)T^{4\nu+2d-1}, \tag{39}$$

where process = {Direct, Stokes, Anti-Stokes, Spont}, $x_D=\hbar\omega_D/k_BT$ is a dimensionless parameter, T is the temperature, and the coefficients $a^{\text{process}}_{m_s,m_s'}$, $b^{\text{process}}_{m_s,m_s'}$, and $c^{\text{process}}_{m_s,m_s'}$ are given in Appendix A. Using $\nu=1/2$ and $d=3$, we obtain the following total two-phonon spin relaxation rate

$$\Gamma_{\text{2-ph}}=\sum_{m_s\neq m_s'}\left(\Gamma^{\text{abs}}_{m_s\to m_s'}+\Gamma^{\text{em}}_{m_s\to m_s'}\right)=A_5T^5+A_6T^6+A_7T^7. \tag{40}$$

This total spin relaxation rate will be relevant for the general solution associated with the physical observable $\langle S_z(t)\rangle$ (see Section V B and Eq. (74)). In Table I, we have shown the different temperature dependence of the spin relaxation rate associated with two-phonon processes in the acoustic limit. We observe that the symmetry of the lattice ν and the dimension of the system d determine the temperature response of the spin-lattice relaxation dynamics of the system at high temperatures.

TABLE I. The table shows the expected temperature dependence of linear and bi-linear spin-phonon interactions considered to first and second order in spin lattice relaxation rate. The bi-linear term to second order is zero. When both linear and bi-linear terms are considered a mixed term appears only to second-order. Last column indicates the temperature scaling for a three-dimensional, non-cubic lattice.

Hamiltonian	First-order	Second-order	$d=3$ $\nu=1/2$
$\hat{H}=\sum_{k,i}\lambda_{ki}\hat{x}_k$	$\coth\left(\frac{\hbar\omega}{k_BT}\right)$	$T^{4\nu+2d-3}$	T^5
$\hat{H}=\sum_{k,k',i}\lambda_{kk',i}\hat{x}_k\hat{x}_{k'}$	$T^{4\nu+2d-1}$	0	T^7
Mixed term	0	$T^{4\nu+2d-2}$	T^6

In summary, by only considering the contribution of acoustic phonons to first and second-order, we see three different temperature scalings of the form (T^s, T^{s+1}, T^{s+2}), where $s=4\nu+2d-3$. We observe $1/T_1\propto T^s$ for a linear second-order Raman-like scattering, $1/T_1\propto T^{s+2}$ for a quadratic first-order Raman-like scattering, and $1/T_1\propto T^{s+1}$ for the mixed term between the linear and quadratic contributions to second order.

C. Two-phonon processes: quasi-localized phonons

Quasi-localized phonons, or vibrational resonances between a single-color-center and lattice vibrations, are good candidates for dissipative processes due to the strong electron-phonon coupling. The NV^- center has a strong electron-phonon coupling associated with vibrational resonances, with a continuum of vibrational modes centered at $\omega_{\rm res}=65$ meV, and a full width at half-maximum of about $\Delta=32$ meV as regularly observed in the phonon-sideband of the NV fluorescence spectrum under optical excitation[13]. Because of the small zero-field splitting constant induced by spin-spin interaction ($D/2\pi=2.87$ GHz or $\hbar D=0.012$ meV), we have $\omega_{\rm res}\gg D$, and therefore, these high-energy phonons can only be present in a two-phonon process associated with the condition $\omega_k-\omega_{k'}=\omega_i$ ($\omega_k\approx\omega_{k'}$). Strong interactions with high energy phonons can be introduced in Orbach-type processes[9]. It is shown experimentally that different NV^- center samples have an activation energy of 73 meV[8], which is close to the vibrational resonance frequency $\omega_{\rm res}=65$ meV. In our formalism, quasi-localized phonons can be phenomenologically modeled by a Lorentzian spectral density function of the form[15,36]

$$J_{\rm Loc}(\omega)=\frac{J_{\rm Loc}}{\pi}\frac{\frac{1}{2}\Delta}{\left(\omega-\omega_{\rm loc}\right)^2+\left(\frac{1}{2}\Delta\right)^2},\qquad 0<\omega<\omega_{\rm max}. \tag{41}$$

In this equation, $J_{\rm Loc}$ is the coupling strength, Δ is a characteristic bandwidth, $\hbar\omega_{\rm max}=168$ meV is the maximum phonon energy in a diamond lattice[37], and $\omega_{\rm loc}$ is the frequency of the localized phonon mode. As a simpler model we can consider the interaction with only one quasi-localized phonon mode ($\Delta\to 0$)

$$\lambda_{k,i}=\lambda_{i,\rm loc}\delta(\omega-\omega_{\rm loc}), \tag{42}$$

where $\lambda_{i,\rm loc}$ is the coupling strength. Using the above equation and calculating the second-order transition rate induced by the linear spin-phonon interaction, we can obtain the following relaxation rate associated with quasi-localized phonons

$$\begin{aligned}\Gamma_{\rm loc}&=A_4\left(1+n(\omega_{\rm loc})\right)n(\omega_{\rm loc})\\&\approx\frac{A_4}{e^{\hbar\omega_{\rm loc}/k_BT}-1},\end{aligned} \tag{43}$$

where A_4 is a constant of units of frequency. The approximation $(1+n(\omega_{\rm loc}))\,n(\omega_{\rm loc})\approx n(\omega_{\rm loc})$ is valid for temperatures below T = 300 K. For such temperatures, the mean number of phonons is low, $n(\omega_{\rm loc})\approx 0.1$, therefore we can write $(1+n)n\approx n+\mathcal{O}(n^2)$.

In the next section we derive the spin-lattice relaxation dynamics using the quantum master equation.

IV. SPIN-LATTICE RELAXATION DYNAMICS

In this section, we present the general equation associated with the spin-lattice relaxation dynamics of the ground triplet state of the NV^- center. We use the Markovian quantum master equation[38] for the reduced density operator $\hat{\rho}(t)=\mathrm{Tr}_{\rm ph}\left(\hat{\rho}_{\rm NV+ph}\right)$. We assume that the initial state at time t_0 is given by the uncorrelated state $\hat{\rho}_{\rm NV+ph}(t_0)=\hat{\rho}_{\rm NV}(t_0)\otimes\hat{\rho_{\rm ph}}(t_0)$ (Born approximation), and that the phonon bath is in thermal equilibrium. In the weak-coupling limit, and using the spin-phonon Hamiltonian given in Eq. (6), we obtain

$$\dot{\hat{\rho}}=\frac{1}{i\hbar}[\hat{H}_{\rm NV},\hat{\rho}]+\mathcal{L}_{\text{1-ph}}\hat{\rho}+\mathcal{L}_{\text{2-ph}}\hat{\rho}+\mathcal{L}_{\rm mag}\hat{\rho}, \tag{44}$$

where the first term in Eq. (44) describes the free dynamics induced by the NV^- center Hamiltonian [Eq. (2)]. The second and third terms are given by

$$\mathcal{L}_{\text{1-ph}}\hat{\rho}=\sum_{i=1}^{3}\left[\Gamma_{\rm abs}^{i,\text{1-ph}}\mathcal{L}[L_+^i]\hat{\rho}+\Gamma_{\rm em}^{i,\text{1-ph}}\mathcal{L}[L_-^i]\hat{\rho}\right], \tag{45}$$

$$\mathcal{L}_{\text{2-ph}}\hat{\rho}=\sum_{i=1}^{3}\left[\Gamma_{\rm abs}^{i,\text{2-ph}}\mathcal{L}[L_+^i]\hat{\rho}+\Gamma_{\rm em}^{i,\text{2-ph}}\mathcal{L}[L_-^i]\hat{\rho}\right], \tag{46}$$

which describe the dissipative spin-lattice dynamics induced by one-phonon and two-phonon processes, with the index $i=1,2,3$ representing the spin transitions of the system (see Fig. 1). In Eqs. (45) and (46) we have defined the Lindblad super-operator $\mathcal{L}[\hat{O}]\hat{\rho}=\hat{O}\hat{\rho}\hat{O}^\dagger-\frac{1}{2}\{\hat{O}^\dagger\hat{O},\hat{\rho}\}$ and the spin operators

$$L_+^1=|m_s=1\rangle\langle m_s=-1|=\left(L_-^1\right)^\dagger, \tag{47}$$

$$L_+^2=|m_s=1\rangle\langle m_s=0|=\left(L_-^2\right)^\dagger, \tag{48}$$

$$L_+^3=|m_s=-1\rangle\langle m_s=0|=\left(L_-^3\right)^\dagger. \tag{49}$$

The last term in Eq. (44) is an extra term that describes a phenomenological dynamics induced by magnetic impurities, and is given by

$$\mathcal{L}_{\rm mag}\hat{\rho} = -\frac{1}{4}\Gamma_{\rm mag}\sum_{i=x,y,z}\left[S_i,[S_i,\hat{\rho}(t)]\right], \tag{50}$$

where $\Gamma_{\rm mag}$ is the magnetic relaxation rate induced by an isotropic magnetic noise[39], and S_i are the Pauli matrices for $S=1$. From previous works, it is expected that the parameter $\Gamma_{\rm mag}$ will proportionally depend on the concentration of neighboring NV^- centers[8] and temperature. Therefore, $\Gamma_{\rm mag}$ is a sample-dependent parameter that models magnetic impurities. The exact temperature dependence of $\Gamma_{\rm mag}$ is beyond the scope of this work, but we expect it to change as temperature reaches $T_{\rm gap} = \hbar D/k_B \approx 0.14$ K. In addition, in this work we neglect the effect of electric field fluctuations. This is relevant for experiments that involve optical illumination and read-out of the electronic states[32].

Now, we study the longitudinal relaxation rate at low and high temperatures. In the low-temperature limit we also investigate the effect of magnetic field on the longitudinal relaxation rate.

V. DISCUSSION

A. Low-temperature limit

In this section we discuss the low-temperature limit (below 1 K) associated to the spin-lattice relaxation dynamics of the ground state of the NV^- center in diamond. For low temperatures, only one-phonon processes contribute to the transition rates. Therefore, we can deduce the spin-lattice dynamics from the quantum master equation by setting $\mathcal{L}_{\text{2-ph}}\hat{\rho}=0$. From Eq. (44) we can find the dynamics of the spin populations $p_1 = \langle m_s=1|\,\hat{\rho}\,|m_s=1\rangle$, $p_2 = \langle m_s=0|\,\hat{\rho}\,|m_s=0\rangle$, and $p_3 = \langle m_s=-1|\,\hat{\rho}\,|m_s=-1\rangle$. For an arbitrary magnetic field B_0 along the z axis, using $\Gamma_{\rm mag}=0$, and considering only one-phonon processes, the equations at low temperatures are given by

$$\frac{{\rm d}p_1}{{\rm d}t} = -\left(\gamma_{+-}+\Omega_{+0}\right)p_1 + \Omega_{0+}p_2 + \gamma_{-+}p_3, \tag{51}$$

$$\frac{{\rm d}p_2}{{\rm d}t} = -\left(\Omega_{0+}+\Omega_{0-}\right)p_2 + \Omega_{+0}p_1 + \Omega_{-0}p_3, \tag{52}$$

$$\frac{{\rm d}p_3}{{\rm d}t} = -\left(\Omega_{0-}+\gamma_{-+}\right)p_3 + \gamma_{+-}p_1 + \Omega_{0-}p_2, \tag{53}$$

where the direct relaxation rates between the spin states are given by $\gamma_{+-} = A_1(1+n_1)$, $\gamma_{-+} = A_1 n_1$, $\Omega_{+0} = A_2(1+n_2)$, $\Omega_{0+} = A_2 n_2$, $\Omega_{-0} = A_3(1+n_3)$, and $\Omega_{0-} = A_3 n_3$ (see Fig. 4), where $n_i = [\exp(\hbar\omega_i/k_BT)-1]^{-1}$ is the mean number of phonons at thermal equilibrium. Here, $\omega_1 = 2\gamma_s B_0$, $\omega_2 = D+\gamma_s B_0$, and $\omega_3 = D-\gamma_s B_0$ are the resonant frequencies associated with the spin energy levels. The A_i parameters are defined in Eqs. (25)-(27) and are estimated as a function of the magnetic field B_0 in the next section [see Eqs. (63)-(65)]. For experiments in quantum information processing and magnetometry these direct relaxation rates play a fundamental role.

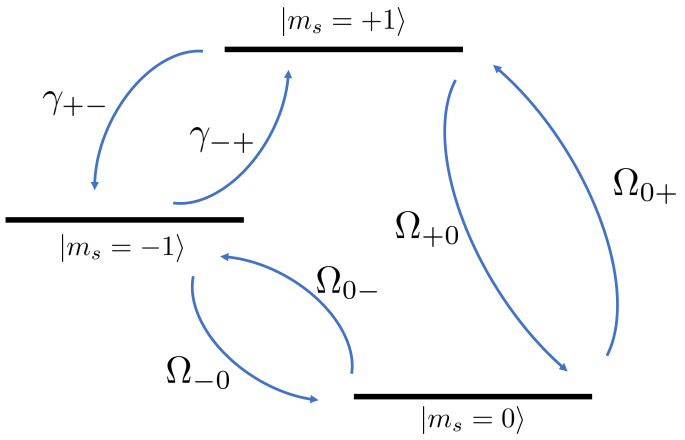

FIG. 4. Direct relaxation rates induced by one-phonon processes. The spin populations associated with the spin states $|m_s=0,\pm1\rangle$ are modified by the absorption $(\gamma_{-+},\Omega_{0-},\Omega_{0+})$ and emission rates $(\gamma_{+-},\Omega_{-0},\Omega_{+0})$. For magnetic fields $\gamma_s B_0 > D$ ($B_0 > 1000$ G), the state $|m_s=-1\rangle$ is the lowest energy state and the role of Ω_{0-} and Ω_{-0} are exchanged.

In the following we obtain the longitudinal relaxation rate for the physical observables $\langle S_z^2(t)\rangle$ and $\langle S_z(t)\rangle$ at different magnetic field regimes. However, this model can be used to determine any other physical observable, for instance, direct relaxation rates between spin states and their magnetic field and temperature dependence.

1. *Zero magnetic field*

At zero magnetic field ($B_0=0$) and neglecting the effect of strain, the spin states $|m_s=1\rangle$ and $|m_s=-1\rangle$ are degenerate (see Fig. 1). As a consequence, the emission and absorption rates associated with the spin transitions $|m_s=0\rangle \leftrightarrow |m_s=1\rangle$ and $|m_s=0\rangle \leftrightarrow |m_s=-1\rangle$ are equal.

Therefore, the system can be modeled as a simple two-level system with the degenerate excited states described by $|m_s=\pm1\rangle$. In addition, the transition rate between $|m_s=\pm1\rangle$ vanishes if we neglect the effect of electric field fluctuations[32]. In such scenario, the absorption and emission rates are given by $\Gamma_{\rm abs} = \Gamma_0\bar{n}$ and $\Gamma_{\rm em} = \Gamma_0(\bar{n}+1)$, respectively, where $\bar{n} = [\exp(\hbar D/k_BT)-1]^{-1}$ is the mean number of phonons at the zero-field splitting frequency $D/2\pi = 2.87$ GHz. The parameter Γ_0 is obtained from Eqs. (26) and (27) for $B_0=0$ and is given by

$$\Gamma_0 = \frac{\Omega D^3(\lambda_{0x'}^2+\lambda_{0y'}^2)}{2\pi v_s^3\omega_D}. \tag{54}$$

From Eqs. (51)-(53), we obtain

$$\frac{\mathrm{d}p_1}{\mathrm{d}t} = \Gamma_0(1+\bar{n})p_1 + \Gamma_0\bar{n}p_2, \tag{55}$$

$$\frac{\mathrm{d}p_2}{\mathrm{d}t} = -2\Gamma_0\bar{n}p_2 + \Gamma_0(1+\bar{n})p_1 + \Gamma_0(1+\bar{n})p_3, \tag{56}$$

$$\frac{\mathrm{d}p_3}{\mathrm{d}t} = \Gamma_0(1+\bar{n})p_1 + \Gamma_0\bar{n}p_3. \tag{57}$$

Using $\langle S_z^2(t)\rangle = p_1(t) + p_3(t)$ and $p_1(t) + p_2(t) + p_3(t) = 1$ we obtain

$$\frac{\mathrm{d}\langle S_z^2(t)\rangle}{\mathrm{d}t} = -\Gamma_0(1+3\bar{n})\langle S_z^2(t)\rangle + 2\Gamma_0\bar{n}, \tag{58}$$

$$\frac{\mathrm{d}p_2}{\mathrm{d}t} = -\Gamma_0(1+3\bar{n})p_2(t) + \Gamma_0(1+\bar{n}). \tag{59}$$

Using arbitrary initial conditions $p_i(0) = p_{i0}$ $(i = 1, 2, 3)$, we have

$$\begin{aligned}\langle S_z^2(t)\rangle &= \langle S_z^2(T)\rangle_{\mathrm{st}} - \left(\langle S_z^2(T)\rangle_{\mathrm{st}} - p_{10} - p_{30}\right) e^{-\Gamma_0(1+3\bar{n})t},\\ p_2(t) &= \left(p_2(T)\right)_{\mathrm{st}} - \left(\left(p_2(T)\right)_{\mathrm{st}} - p_{20}\right) e^{-\Gamma_0(1+3\bar{n})t},\end{aligned} \tag{60}$$

where the steady states are given by

$$\langle S_z^2(T)\rangle_{\mathrm{st}} = \frac{2}{e^{\hbar D/k_BT} + 2}, \tag{61}$$

$$\left(p_2(T)\right)_{\mathrm{st}} = \frac{e^{\hbar D/k_BT}}{e^{\hbar D/k_BT} + 2}. \tag{62}$$

Therefore, the phonon-induced spin relaxation rate associated with $\langle S_z^2(t)\rangle$ and $p_2(t)$ (ground state population) are given by $1/T_1 = \Gamma_0(1+3\bar{n})$. In order to compare our model to real systems, we extract the value of Γ_0 from recent experimental results[12] which is $\Gamma_0 = 3.14 \times 10^{-5}$ s^{-1} (see Fig. 5a). Using Eq. (54) and assuming $\lambda_{0x'} \approx \lambda_{0y'} \approx \lambda_{0x} \approx \lambda_{0y}$, we estimate $\lambda_{0x'}$ to be approximately 78.38 GHz. We note that other recent experimental results seem to suggest an order of magnitude smaller values for Γ_0[33]. Nevertheless, with this approximation for the λ_0 factors and combining Eqs. (25)-(27) with Eq. (54), we can estimate the following magnetic field dependence for the one-phonon spin relaxation rates

$$A_1 \approx 2\Gamma_0\left(\frac{2\gamma_sB_0}{D}\right)^3, \tag{63}$$

$$A_2 \approx \Gamma_0\left[\frac{(D+\gamma_sB_0)}{D}\right]^3, \tag{64}$$

$$A_3 \approx \Gamma_0\left[\frac{(D-\gamma_sB_0)}{D}\right]^3. \tag{65}$$

Note that $\langle S_z(t)\rangle$ is zero as the states $|m_s = +1\rangle$ and $|m_s = -1\rangle$ are degenerate at zero magnetic field. In the next section we introduce the effect of low magnetic field on the longitudinal relaxation rate associated with $\langle S_z(t)\rangle$.

2. Low magnetic field

We define the limit of low magnetic fields when $\gamma_sB_0 \ll D$ so that $n(D+\gamma_sB_0) \approx n(D-\gamma_sB_0) \approx \bar{n}$. By considering one-phonon processes, we obtain the following set of equations

$$\frac{\mathrm{d}\langle S_z^2(t)\rangle}{\mathrm{d}t} = -\Gamma_0(1+3\bar{n})\langle S_z^2(t)\rangle + 3\epsilon\Gamma_0(1+\bar{n})\langle S_z(t)\rangle + 2\Gamma_0\bar{n}, \tag{66}$$

$$\frac{\mathrm{d}\langle S_z(t)\rangle}{\mathrm{d}t} = -\left[\Gamma_Bn_B + 3\epsilon\Gamma_0(1+3\bar{n})\right]\langle S_z^2(t)\rangle + 6\epsilon\Gamma_0\bar{n} - \left[\Gamma_B(1+2n_B) + \Gamma_0(1+\bar{n})\right]\langle S_z(t)\rangle, \tag{67}$$

where $\epsilon = \gamma_sB_0/D \ll 1$ is a pertubative dimensionless parameter, $\Gamma_B \approx \Gamma_0(2\gamma_sB_0/D)^3$, and $n_B = \left[\exp(2\hbar\gamma_sB_0/k_BT) - 1\right]^{-1}$ is the mean number of phonons at the resonant frequency $\omega_1 = 2\gamma_sB_0$. In addition, the mean number of phonons satisfies $n_B \gg \bar{n}$ due to the condition $\gamma_sB_0 \ll D$.

At low magnetic fields, the longitudinal relaxation rate associated with $\langle S_z(t)\rangle$ is given by

$$\frac{1}{T_1} \approx 2\Gamma_0(1+2\bar{n}) + \Gamma_B(1+2n_B). \tag{68}$$

The steady states satisfy the relation

$$\frac{\langle S_z^2(T)\rangle_{\mathrm{st}}}{\langle S_z(T)\rangle_{\mathrm{st}}} = \frac{\Gamma_0(1+\bar{n}) + \Gamma_B(1+2n_B)}{n_B\Gamma_B}. \tag{69}$$

In the next section we obtain the longitudinal relaxation rate associated with $\langle S_z(t)\rangle$ for arbitrary values of the magnetic field B_0.

3. Arbitrary magnetic field values

At non-zero magnetic fields, the spin states $|m_s = -1\rangle$ and $|m_s = 1\rangle$ are split due to the Zeeman interaction (see Fig. 1). This implies that the system can be modeled as a dissipative three-level system consisting of the spin states $|m_s = 0\rangle$ and $|m_s = \pm 1\rangle$. From Eqs. (51)-(53), the dynamics for the longitudinal spin component is given by

$$\frac{\mathrm{d}^2\langle S_z(t)\rangle}{\mathrm{d}t^2} + \frac{1}{T_1}\frac{\mathrm{d}\langle S_z(t)\rangle}{\mathrm{d}t} + \omega^2\langle S_z(t)\rangle = A_0, \tag{70}$$

where the parameters are given by

$$\frac{1}{T_1} = A_1(1+2n_1) + A_2(1+2n_2) + A_3(1+2n_3), \tag{71}$$

$$\begin{aligned}\omega^2 = \frac{1}{2}\big\{&A_1[A_3(1+n_3) - A_2(1+n_2)] - A_2^2n_2(3+n_2)\\ &-A_3^2n_3(3+n_3) + A_2A_3(2+n_2+n_3+4n_2n_3)\big\},\end{aligned}$$

$$\begin{aligned}A_0 = \frac{1}{2}\big[&2A_1(A_2+A_3) + A_2^2(1+n_2)^2\\ &+2A_2A_3(n_2-n_3) - A_3^2(1+n_3)^2\big].\end{aligned} \tag{72}$$

We observe that the relaxation rate $1/T_1$ is given by the total one-phonon spin relaxation rate given in Eq. (21). The general solution is that of a driven damped harmonic oscillator, where the longitudinal relaxation rate is given by

$$\frac{1}{T_1} \approx \frac{\Gamma_0}{D^3}\omega_1^3(1+2n_1) + \frac{\Gamma_0}{D^3}\left[\omega_2^3(1+2n_2) + \omega_3^3(1+2n_3)\right], \tag{73}$$

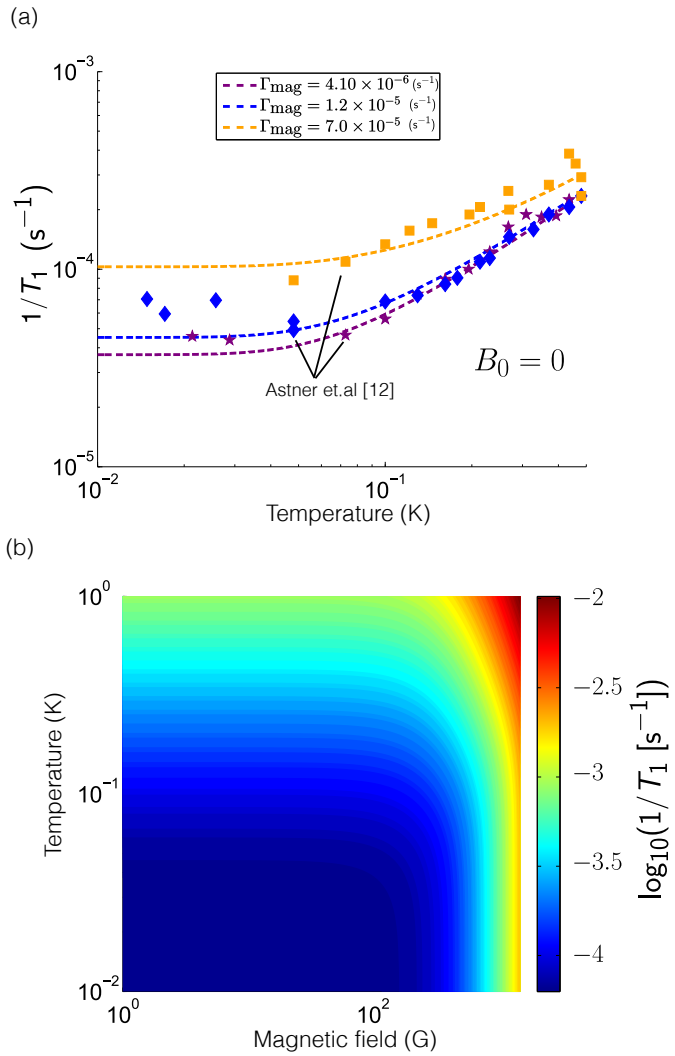

FIG. 5. (a) Relaxation rate of $\langle S_z^2(t)\rangle$ at zero magnetic field. The symbols represent experimental spin relaxation rates measured at low temperatures (below 1 K) for different NV-samples (Astner et. al.[12]). The dotted lines represent the theoretical fit given by $1/T_1 = \Gamma_0(1+3\bar{n})+\Gamma_{\rm mag}$. We observe that at low temperatures, the relevant contribution comes from the emission of a phonon and the magnetic noise induced by the environment. (b) Two-dimensional parameter plot of the longitudinal relaxation rate of $\langle S_z(t)\rangle$ in logarithm scale at magnetic fields ranging from 0 to 1500 G, temperature ranging from 10 mK to 1 K, and $\Gamma_{\rm mag} = 0$.

where $\omega_1 = 2\gamma_s B_0$, $\omega_2 = D+\gamma_s B_0$, and $\omega_3 = D-\gamma_s B_0$. In this approximation we have assumed that $\lambda_{0x'}^2 + \lambda_{0y'}^2 \approx \lambda_{0x}^2 + \lambda_{0y}^2$ (see Eqs. (25)-(27)). At low magnetic fields, $\gamma_s B_0 \ll D$, we recover the previous result given in Eq. (68). Figure. 5b shows the expected longitudinal relaxation rate at low temperatures for magnetic fields ranging from 0 to 1500 G. As the magnetic field increases, the longitudinal relaxation rate increases as well.

B. High-temperature limit

In this section, we consider higher temperatures for which the relaxation rate is dominated by quasi-localized phonons and two-phonon processes, usually for temperatures higher than 100 K. By solving the quantum master equation we obtain that the longitudinal spin relaxation rate of $\langle S_z(t)\rangle$ (see Appendix B) is approximately given by

$$\begin{aligned}\frac{1}{T_1} &\approx \Gamma_{\rm mag} + \Gamma_{\text{1-ph}} + \Gamma_{\rm loc} + \Gamma_{\text{2-ph}},\\ &= \Gamma_{\rm mag} + \sum_{i=1}^{3} A_i \coth\left(\frac{\hbar\omega_i}{k_B T}\right) + \frac{A_4}{e^{\hbar\omega_{\rm loc}/k_B T}-1}\\ &\quad + A_5 T^5 + A_6 T^6 + A_7 T^7. \end{aligned} \tag{74}$$

In the above equation, $\omega_1 = 2\gamma_s B_0$, $\omega_2 = D+\gamma_s B_0$, and $\omega_3 = D-\gamma_s B_0$ are the resonant frequencies of the ground triplet states of the NV$^-$ center in diamond in the presence of the static magnetic field B_0 along the z axis, and T is the temperature. Similar formulas for the longitudinal relaxation rate were obtained phenomenologically in order to fit the experimental data for different NV$^-$ center samples[8,9]. However, our work formally incorporates the phonon-induced spin relaxation rates by including the contribution of stochastic magnetic noise, direct one-phonon processes, strong interactions with quasi-localized phonon modes, and the effect of the acoustic phonons to first and second order. This is crucially different from previous works[8,9,11,12], but validates, both high and low-temperature experimental observations in which electric field fluctuations is not present (see Fig. 6). Our model can also be useful to understand the temperature dependence of the longitudinal spin relaxation rate of other color centers in diamond. For instance, it is consistent with the observed T^7 temperature dependence of the neutral silicon-vacancy color center in diamond at high temperatures[41].

Using experimental data from Refs.[8,12], we can fit our free parameter $\Gamma_{\rm mag}$ in order to model the magnetic noise induced by magnetic impurities in samples with different NV$^-$ concentrations. On the other hand, we consider that the A_i parameters, which are related to the spin-phonon coupling constants, are not sample-dependent. The A_1, A_2, and A_3 parameters can be found by fitting to the experimental data at low temperature (below 1 K)[12] as described in Sec. V A. The parameters A_4, A_5, A_6, A_7, and $\omega_{\rm loc}$ can be found by fitting to the experimental data for temperatures ranging from 4 K to 475 K[8].

Figure 6 shows the temperature dependence of the longitudinal relaxation rate for different samples at high temperatures. For the two-phonon processes we obtain $A_4 = 1.96(5)\times 10^{-3}$ s^{-1}, $A_5 = 2.06(5)\times 10^{-11}$ s^{-1} K^{-5}, $A_6 = 9.11(2)\times 10^{-16}$ s^{-1} K^{-6}, $A_7 = 2.55(3)\times 10^{-20}$ s^{-1} K^{-7}, and $\omega_{\rm loc} = 73(5)$ meV. We observe a good agreement between our results and the experiments performed at high temperatures[8,9,11]. The largest contribution at high temperatures, 300 K $< T <$ 500 K, is due to the second-order scattering (see Table I and Fig. 3) usually known as the second-order Raman scattering[19] which leads to the ob-

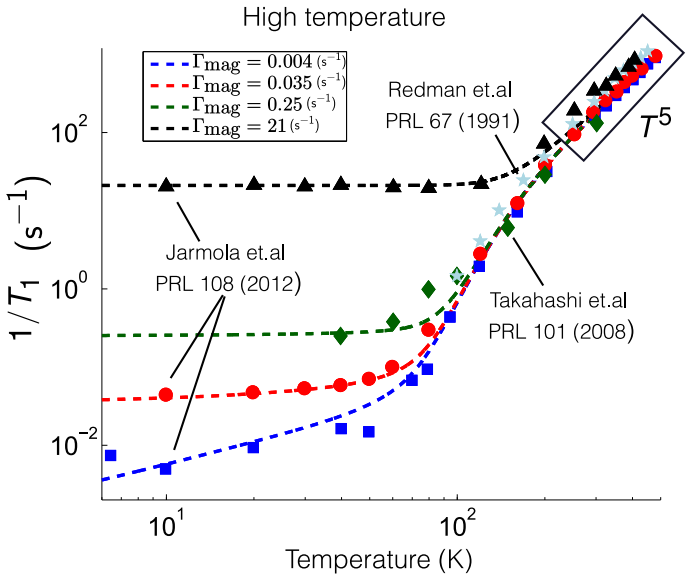

FIG. 6. The symbols represent experimental spin relaxation rates measured for different NV^- samples in the temperature regime 4-475 K[8,9,11]. The dotted lines are the theoretical fit of the longitudinal spin relaxation rate $1/T_1$ given in Eq. (74) for different values of the magnetic noise $\Gamma_{\rm mag}$. The temperature at which the contribution from quasi-localized phonons and second-order phonon processes dominates is sample dependent.

served $1/T_1 \propto T^5$ temperature dependence[8,9,11] due to the linear spin-phonon coupling to second-order. Between 50 K $< T <$ 200 K the main contribution arises from Orbach-type processes[20] which can be attributed to a strong spin-phonon interaction with a quasi-localized phonon mode with energy ≈ 73 meV[8]. On the other hand, the magnetic noise rate $\Gamma_{\rm mag}$ is dominant in samples with a high NV concentration (red, green and black dashed curves in Fig. 6). Therefore, the effect of one-phonon processes (emission and absorption) can be neglected if the magnetic noise is larger than the one-phonon spin relaxation rates. We note that we are not considering other sources of relaxation such as fluctuating electric fields, in which case a relaxation with an inverse magnetic field dependence is expected[32].

VI. CONCLUSIONS

In summary, we have presented a microscopic model for estimating the effect of temperature on the longitudinal relaxation rate $1/T_1$ of NV^- centers in diamond. In this model, we introduced a general spin-phonon interaction between the ground-state spin degree of freedom and lattice vibrations. We estimated the value of the phonon-induced spin relaxation rates by applying the Fermi golden rule to first and second order. The microscopic spin-lattice relaxation dynamics was derived from the quantum master equation for the reduced spin density operator. In the relaxation dynamics, we included the effect of a phononic bath in thermal equilibrium and phenomenologically modeled magnetic impurities. Acoustic and quasi-localized phonons were included in the phonon processes in order to model a more general temperature dependence of the longitudinal relaxation rate.

At low temperatures, we provided a set of microscopic equations in order to study the spin-lattice relaxation dynamics induced by one-phonon processes. In this limit and considering zero magnetic fields, $B_0 = 0$, we analytically obtained the relaxation rate $1/T_1 = \Gamma_0(1 + 3\bar{n})$ associated with $\langle S_z^2(t)\rangle$, where Γ_0 depends on microscopic constants. This relaxation rate is in agreement with recent experiments and *ab initio* calculations[8], as well as theoretical calculations[40]. In addition, for low magnetic fields, $\gamma_s B_0 \ll D$, we obtained the relaxation rate $1/T_1 = 2\Gamma_0(1 + 2\bar{n}) + \Gamma_B(1 + 2n_B)$ associated with $\langle S_z(t)\rangle$, where Γ_B scales as B_0^3.

At high temperatures, we have modeled multiple two-phonon processes where the fitted relaxation rate associated to $\langle S_z(t)\rangle$ is in agreement with experimental observations[8,9,11]. We included both linear and bi-linear lattice interactions that lead to several different temperature scaling in a spin-boson model. In particular, for NV-centers in diamond the dominant temperature scaling is T^5 for temperatures larger than 200 K. Moreover, our model will be useful to evaluate the contribution of second-order phonon processes that give different temperature scaling (T^s, T^{s+1}, T^{s+2}) for other spin-boson systems. The power of the temperature $s = 4\nu + 2d - 3$ depends on the dimension of the system and the symmetry of the lattice, where $d = 3$ and $\nu = 1/2$ for the NV^- center.

VII. ACKNOWLEDGEMENTS

The authors acknowledge the CONICYT UC Berkeley-Chile collaboration program. A.N. acknowledges support from Conicyt fellowship and Gastos Operacionales of Conicyt No. 21130645. E.M. acknowledges support from Conicyt-Fondecyt 1141146. H.T.D. acknowledges support from Fondecyt-Postdoctoral Grant No. 3170922. D.B. acknowledges support by the DFG through the DIP program (FO 703/2-1). J.R.M. acknowledges support from Conicyt-Fondecyt 1141185, Conicyt-PIA ACT1108, and AFOSR grant FA9550-16-1-0384.

Appendix A: Fermi golden rule

In this section we derive the analytic form of the second-order phonon-induced spin relaxation rates introduced in Sec. III B. To second order in time-dependent perturbation theory the transition rate between an initial $|i\rangle$ and final state $|f\rangle$ is given by

$$\Gamma_{i\to f} = \frac{2\pi}{\hbar}\left| V_{fi} + \sum_m \frac{V_{fm}V_{mi}}{E_i - E_m}\right|^2 \delta(E_i - E_f), \qquad \text{(A1)}$$

where $V_{ij} = \langle i|\,\hat{H}_{\text{s-ph}}\,|j\rangle$, with $\hat{H}_{\text{s-ph}}$ being the perturbation. In Eq. (A1) the sum over m denotes all possible intermediate states $|m\rangle$ for which $V_{fm}V_{mi} \neq 0$. Here, E_i,

E_f, and E_m are the energies of the initial, final, and intermediate states, respectively. For the Stokes transition the initial and final states are given by $|i\rangle = |m_s, n_k, n_{k'}\rangle$ and $|f\rangle = |m'_s, n_k - 1, n_{k'} + 1\rangle$. Let us write the spin-phonon Hamiltonian given in Eq. (6) as $\hat{H}_{\text{s-ph}} = V^{(1)} + V^{(2)}$ with $V^{(1)} = \sum_i \sum_{k\in\Gamma_i} \lambda_{k,i}(\hat{b}_k + \hat{b}_k^\dagger)\hat{F}_i(\mathbf{S})$ and $V^{(2)} = \sum_i \sum_{k\otimes k'\in\Gamma_i} \lambda_{kk',i}(\hat{b}_k + \hat{b}_k^\dagger)(\hat{b}_{k'} + \hat{b}_{k'}^\dagger)\hat{F}_i(\mathbf{S})$ being the linear and quadratic spin-phonon interactions, respectively. It is straightforward to verify that $V^{(2)}_{fm}V^{(2)}_{mi} = V^{(1)}_{fm}V^{(2)}_{mi} = V^{(2)}_{fm}V^{(1)}_{mi} = 0$ for every intermediate state $|m\rangle$ with initial and final states for Stokes transition, i.e., $|i\rangle = |m_s, n_k, n_{k'}\rangle$ and $|f\rangle = |m'_s, n_k - 1, n_{k'} + 1\rangle$. In other words, the contribution of the quadratic term $V^{(2)}$ is zero to second order. This implies that lower order perturbation theory combined with higher order phonon coupling wins over higher order perturbatin theory with lower order coupling[21]. Similar arguments can be applied to the other two-phonon processes.

The non-zero contributions to the transition rate can be obtained if we expand the phonon part of the summation for the intermediate states $|n_p, n_{p'}\rangle = \{|n_k - 1, n_{k'}\rangle, |n_k, n_{k'} + 1\rangle\}$, we obtain

$$\Gamma^{m'_s,n_k-1,n_{k'}+1}_{m_s,n_k,n_{k'}} = \frac{2\pi}{\hbar} n_k(n_{k'}+1)\left|\sum_i g_i^{m'_s,m_s}\lambda_{kk',i} + \frac{1}{\hbar}\sum_{m''_s}\sum_{i,j}\lambda_{k',i}\lambda_{k,j}\left(\frac{g_i^{m'_s,m''_s}g_j^{m''_s,m_s}}{\omega_k} - \frac{g_i^{m''_s,m_s}g_j^{m'_s,m''_s}}{\omega_{k'}}\right)\right|^2 \times\delta(\omega_{m'_s,m_s} - \omega_k + \omega_{k'}), \tag{A2}$$

where $g_i^{m_s,m'_s} = \langle m_s|\,\hat{F}_i(\mathbf{S})\,|m'_s\rangle$, and the summation over i and j is over x, y, x', y', z. Here, we have used the approximation $\omega_{k,k'} \gg \omega_{m_s,m''_s}$. By taking the continuous limit and using the density of phonon states given in Eq. (23) we obtain

$$a^{\text{Stokes}}_{m_s,m'_s}(x_D) = \frac{2\pi D_0^2}{\hbar^3\omega_D^{4\nu+2d-2}}\int_0^{x_D} n(x)(n(x - x_{m'_s,m_s}) + 1)x^{2\nu+d-1}(x - x_{m'_s,m_s})^{2\nu+d-1} \times\left|\sum_{m''_s}\sum_{i,j}\lambda_{0i}\lambda_{0j}\left(\frac{g_i^{m'_s,m''_s}g_j^{m''_s,m_s}}{x} - \frac{g_i^{m''_s,m_s}g_j^{m'_s,m''_s}}{(x - x_{m'_s,m_s})}\right)\right|^2 dx, \tag{A3}$$

$$b^{\text{Stokes}}_{m_s,m'_s}(x_D) = \frac{2\pi D_0^2}{\hbar^2\omega_D^{4\nu+2d-2}}\int_0^{x_D} n(x)(n(x - x_{m'_s,m_s}) + 1)x^{2\nu+d-1}(x - x_{m'_s,m_s})^{2\nu+d-1} \times 2\text{Re}\left[\sum_{m''_s}\sum_i\sum_{i',j'}\lambda_{00i}\lambda_{0i'}\lambda_{0j'}\left(\frac{g_{i'}^{m'_s,m''_s}g_{j'}^{m''_s,m_s}}{x} - \frac{g_{i'}^{m''_s,m_s}g_{j'}^{m'_s,m''_s}}{(x - x_{m'_s,m_s})}\right)\right] dx, \tag{A4}$$

$$c^{\text{Stokes}}_{m_s,m'_s}(x_D) = \frac{2\pi D_0^2\left|\sum_i g_i^{m'_s,m_s}\lambda_{00i}\right|^2}{\hbar\omega_D^{4\nu+2d-2}}\int_0^{x_D} n(x)(n(x - x_{m'_s,m_s}) + 1)x^{2\nu+d-1}(x - x_{m'_s,m_s})^{2\nu+d-1}\,dx. \tag{A5}$$

where for a three dimensional lattice $D_0 = \Omega\omega_D^2/(2\pi v_s^3)$, ω_D is the Debye frequency, d is the dimension of the lattice, ν is the scaling of the spin-phonon coupling for acoustic phonons [see Eq. (22)]. Here, $x_D = \hbar D/(k_B T)$, $x_{m'_s,m_s} = \hbar\omega_{m'_s,m_s}/(k_B T)$, in which $\omega_{m'_s,m_s} = \omega_{m'_s} - \omega_{m_s}$, k_B is the Boltzmann constant, $\hbar$ is the Planck constant, and T is the temperature. Similar formulas can be obtained for the other processes (Direct, Anti-Stokes and Spontaneous emission).

Appendix B: Quantum master equation

In this section we solve the quantum master equation for the ground state spin degree of freedom of the NV$^-$ center in diamond. By solving the quantum master equation given in Eq. (44), for the spin populations $p_1 = \langle m_s = 1|\,\hat{\rho}\,|m_s = 1\rangle$, $p_2 = \langle m_s = 0|\,\hat{\rho}\,|m_s = 0\rangle$, and $p_3 = \langle m_s = -1|\,\hat{\rho}\,|m_s = -1\rangle$, we obtain

$$\dot{p}_1 = -\Gamma'_1 p_1 + \Gamma'_2 p_2 + \Gamma_3 p_3, \tag{B1}$$

$$\dot{p}_2 = -\Gamma'_4 p_2 + \Gamma'_5 p_1 + \Gamma'_6 p_3,$$

$$\dot{p}_3 = -\Gamma'_7 p_3 + \Gamma_8 p_1 + \Gamma'_9 p_2, \tag{B2}$$

where $\Gamma_i' = \Gamma_i + \Gamma_{\rm mag}/2$, and the phonon-induced spin relaxation rates are given by

$$\Gamma_1 = \Gamma_{\rm em}^{1,1\text{-ph}} + \Gamma_{\rm em}^{1,2\text{-ph}} + \Gamma_{\rm em}^{2,1\text{-ph}} + \Gamma_{\rm em}^{2,2\text{-ph}}, \quad \text{(B3)}$$
$$\Gamma_2 = \Gamma_{\rm abs}^{2,1\text{-ph}} + \Gamma_{\rm abs}^{2,2\text{-ph}}, \quad \text{(B4)}$$
$$\Gamma_3 = \Gamma_{\rm abs}^{1,1\text{-ph}} + \Gamma_{\rm abs}^{1,2\text{-ph}}, \quad \text{(B5)}$$
$$\Gamma_4 = \Gamma_{\rm abs}^{2,1\text{-ph}} + \Gamma_{\rm abs}^{2,2\text{-ph}} + \Gamma_{\rm abs}^{3,1\text{-ph}} + \Gamma_{\rm abs}^{3,2\text{-ph}}, \quad \text{(B6)}$$
$$\Gamma_5 = \Gamma_{\rm em}^{2,1\text{-ph}} + \Gamma_{\rm em}^{2,2\text{-ph}}, \quad \text{(B7)}$$
$$\Gamma_6 = \Gamma_{\rm em}^{3,1\text{-ph}} + \Gamma_{\rm em}^{3,2\text{-ph}}, \quad \text{(B8)}$$
$$\Gamma_7 = \Gamma_{\rm abs}^{1,1\text{-ph}} + \Gamma_{\rm abs}^{1,2\text{-ph}} + \Gamma_{\rm em}^{3,1\text{-ph}} + \Gamma_{\rm em}^{3,2\text{-ph}}, \quad \text{(B9)}$$
$$\Gamma_8 = \Gamma_{\rm em}^{1,1\text{-ph}} + \Gamma_{\rm em}^{1,2\text{-ph}}, \quad \text{(B10)}$$
$$\Gamma_9 = \Gamma_{\rm abs}^{3,1\text{-ph}} + \Gamma_{\rm abs}^{3,2\text{-ph}}. \quad \text{(B11)}$$

where $\Gamma_1 = \Gamma_5 + \Gamma_8$, $\Gamma_4 = \Gamma_2 + \Gamma_9$, and $\Gamma_7 = \Gamma_3 + \Gamma_6$, which implies that $\dot{p}_1 + \dot{p}_2 + \dot{p}_3 = 0$, and therefore, $\mathrm{Tr}(\hat{\rho}) = 1$. The analytic solution for the populations $p_i(t)$ are determined by the following general solution

$$\begin{pmatrix} p_1(t) \\ p_2(t) \\ p_3(t) \end{pmatrix} = \sum_{i=1}^{3} C_i \mathbf{v}_i e^{\lambda_i t}, \quad \text{(B12)}$$

where $\mathbf{v}_i$ and λ_i are the eigenvectors and eigenvalues associated to the set of coupled linear equations of motions given by Eqs. (B1)-(B2). The eigenvalues are given by

$$\lambda_1 = -\frac{1}{2}\left[\Gamma_{\rm mag} + \Gamma_{\rm ph} + \sqrt{\Delta}\right], \quad \text{(B13)}$$
$$\lambda_2 = -\frac{1}{2}\left[\Gamma_{\rm mag} + \Gamma_{\rm ph} - \sqrt{\Delta}\right], \quad \text{(B14)}$$
$$\lambda_3 = 0, \quad \text{(B15)}$$

where

$$\Gamma_{\rm ph} = \Gamma_1 + \Gamma_2 + \Gamma_7 = \sum_{i=1}^{3}\left(\Gamma_{\rm abs}^{i} + \Gamma_{\rm ems}^{i}\right), \quad \text{(B16)}$$

is the total phonon-induced spin relaxation rate, and

$$\begin{aligned}\Delta = {} & \Gamma_{\rm mag}^2 + 2\Gamma_{\rm mag}(\Gamma_9 - \Gamma_8) + \Gamma_2^2 + \Gamma_3^2 + (\Gamma_1 - \Gamma_6 - \Gamma_9)^2 \\ & -2\Gamma_2(\Gamma_7 - \Gamma_5 + \Gamma_8 - \Gamma_9 - \Gamma_{\rm mag}) \\ & -2\Gamma_3(\Gamma_5 - \Gamma_6 - \Gamma_8 + \Gamma_9 + \Gamma_{\rm mag}). \end{aligned} \quad \text{(B17)}$$

If we consider the initial condition $\rho_{00}(0) = 1$ (ground state) and considering that $\langle S_z(t)\rangle \to 0$ when $t \to \infty$, we finally obtain

$$\langle S_z(t)\rangle = e^{-\left(\Gamma_{\rm mag} + \Gamma_{\rm ph}\right)t}\sinh(\Delta t) \propto e^{-t/T_1}. \quad \text{(B18)}$$

Therefore, by assuming that $\left(2\Gamma_{\rm mag} + \Gamma_{\rm ph}\right)/2 > \Delta$, we can recover the longitudinal relaxation rate given in Eq. (74).

[1] J. R. Maze, P. L. Stanwix, J. S. Hodges, S. Hong, J. M. Taylor, P. Cappellaro, L. Jiang, M. V. Gurudev Dutt, E. Togan, A. S. Zibrov, A. Yacoby, R. L. Walsworth, and M. D. Lukin, Nature **455** (2008).

[2] A. Ajoy, U. Bissbort, M.D. Lukin, R.L. Walsworth, and P. Cappellaro, Phys. Rev. X **5**, 011001 (2015).

[3] C. C. Fu, H. Y. Lee, K. Chen, T. S. Lim, H. Y. Wu, P. K. Lin, P. K. Wei, P. H. Tsao, H. C. Chang, and W. Fann, Proc. Natl. Acad. Sci. U.S.A. **104**, 727 (2007).

[4] O. Faklaris, V. Joshi, T. Irinopoulou, P. Tauc, M. Sennour, H. Girard, C. Gesset, J. C. Arnault, A. Thorel, J. P. Boudou, P. A. Curmi, and F. Treussart, ACS Nano **3**, 3955 (2009).

[5] L. P. MacGuinness, Y. Yan, A. Stacey, D. A. Simpson, L. T. Hall, D. Maclaurin, S. Prawer, P. Mulvaney, J. Wrachtrup, F. Caruso, R. E. Scholten, L. C. L. Hollenberg, Nature Nanotechnology **6**, 358 (2011).

[6] B. Naydenov, F. Jelezko (2014) Single-Color Centers in Diamond as Single-Photon Sources and Quantum Sensors. In: Kapusta P., Wahl M., Erdmann R. (eds) Advanced Photon Counting. Springer Series on Fluorescence (Methods and Applications), vol 15. Springer, Cham.

[7] G. D. Fuchs, G. Burkard, P. V. Klimov, and D. D. Awschalom, Nature Physics **7**, 789793 (2011).

[8] A. Jarmola, V. M. Acosta, K. Jensen, S. Chemerisov, and D. Budker, Phys. Rev. Lett. **108**, 197601 (2012).

[9] D. A. Redman, S. Brown, R. H. Sands, and S. C. Rand, Phys. Rev. Lett. **67**, 3420 (1991).

[10] J. Harrison, M. J. Sellars, and N. B. Mason, Diam. Relat. Mater. **15**, 586 (2006).

[11] S. Takahashi, R. Hanson, J. van Tol, M. S. Sherwin, and D. D. Awschalom, Phys. Rev. Lett. **101**, 047601 (2008).

[12] T. Astner, J. Gugler, A. Angerer, S. Wald, S. Putz, N. J. Mauser, M. Trupke, H. Sumiya, S. Onoda, J. Isoya, J. Schmiedmayer, P. Mohn, J. Majer, Nature Materials doi:10.1038/s41563-017-0008-y.

[13] A. Alkauskas, B. B. Buckley, D. D. Awschalom, and C. G. Van de Walle, New. J. Phys. **16**, 073026 (2014).

[14] E. Londero, G. Thiering, A. Gali, and A. Alkauskas, arXiv:1605.02955v2.

[15] A. Norambuena, S. A. Reyes, José Mejía-Lopéz, A.Gali, and J. R. Maze, Phys. Rev. B **94**, 134305 (2016).

[16] M. W. Doherty, F. Dolde, H. Fedder, F. Jelezko, J. Wrachtrup, N. B. Manson, and L. C. L. Hollenberg, Phys. Rev. B **85**, 205203 (2012)

[17] M. W. Doherty, N. B. Manson, P. Delaney, F. Jelezko, J. Wrachtrup, and L. C. Hollenberg, Phys. Rep. **528**, 145 (2013).

[18] J. H. Vleck, Phys. Rev. **57**, 426 (1940).
[19] M. B. Walker, Can. J. Phys. **46**, 1347 (1968).
[20] A. Abragam and B. Bleaney, *Electron Paramagnetic Resonance of Transitions Ions* (Clarendon Press, Oxford, 1970), Chap. 1.11.
[21] S. A. Egorov and J. L. Skinner, The Journal of Chemical Physics **103**, 1533 (1995).
[22] V. Ivády, T. Simon, J. R. Maze, I. Abrikosov, and A. Gali, Phys. Rev. B **90**, 235205 (2014).
[23] M. W. Doherty, V. M. Acosta, A. Jarmola, M. S. J. Barson, N. B. Manson, D. Budker, and L. C. L. Hollenberg, Phys. Rev. B **90**, 041201 (2014).
[24] V. M. Huxter, T. A. A. Oliver, D. Budker, and G. R. Fleming, Nature Physics **9**, 744 (2013).
[25] A. Gali, M. Fyta, and E. Kaxiras, Phys. Rev. B **77**, 155206 (2008).
[26] J. A. Larsson and P. Delaney, Phys. Rev. B **77**, 165201 (2008).
[27] J. H. N. Loubser and J. A. van Wyk, Rep. Prog. Phys. **41**, 1201 (1978).
[28] P. Pavone, K. Karch, O. Schütt, W. Windl, D. Strauch, P. Giannozzi and S. Baroni, Phys. Rev. B **48**, 3156 (1993).
[29] J. P. Goss, R. Jones, S. J. Breuer, P. R. Briddon and S. Öberg, Phys. Rev. Lett. **77**, 3041 (1996).
[30] K. A. Mueller, Phys. Rev. **171**, 350 (1968).
[31] Charles P. Poole, *Encyclopedic Dictionary of Condensed Matter Physics* (Elsevier, San Diedo, Vol 1, 2004).
[32] B. A. Myers, A. Ariyaratne, and A. C. Bleszynski Jayich, Phys. Rev. Lett. **118**, 197201 (2017).
[33] Mohamed H. Abobeih, Julia Cramer, Michiel A. Bakker, Norbert Kalb, Daniel J. Twitchen, Matthew Markham, and Tim H. Taminiau, arXiv:1801.01196v1.
[34] Ulrich Weiss, *Quantum Dissipative Systems* (World Scientific,Third Edition, 2008), Chap. 4.
[35] R. Stedman, L. Almqvist, and G. Nilson, Phys. Rev. **162**, 549 (1967).
[36] M. Thorwart, L. Hartmann, I. Goychuk, and P. Hänggi, J. Mod. Opt. **47**, 2905 (2000).
[37] M. A. Zaitsev, *Optical Properties of Diamond: A Dara Handbook* (Springer-Verlag Berlin Heidelberg, Berlin Heidelberg, Ed. 1, 2011).
[38] H. P. Breuer and F. Petruccione, *The theory of open quantum systems* (Oxford University Press, New York, 2002).
[39] J. E. Avron, O. Kenneth, A. Retzker, and M. Shalyt, New. J. Phys. **17**, 043009 (2015).
[40] P. L. Scott and C. D. Jeffries, Phys. Rev. **127**, 32 (1962).
[41] B.L. Green, S. Mottishaw, B.G. Breeze, A.M. Edmonds, U.F.S. D'Haenens-Johansson, M.W. Doherty, S.D. Williams, D.J. Twitchen, and M.E. Newton, Phys. Rev. Lett. **119**, 096402 (2017).